

CrossMark  
click for updatesCite this: *Chem. Sci.*, 2016, 7, 3836

## Modulating the cobalt redox potential through imidazole hydrogen bonding interactions in a supramolecular biomimetic protein-cofactor model†

Marjorie Sonnay, Thomas Fox, Olivier Blacque and Felix Zelder\*

A realistic model for the active site of histidine-on cobalamin@protein complexes is reported and studied under homogeneous and immobilized conditions. Analysis of lower ligand modulation and its influence on the properties of the biomimetic compound are presented. The cofactor attachment by a protein's histidine residue was imitated by covalently linking an artificial imidazole-containing linker to cobyrinic acid. The resulting intramolecular coordination complex is an excellent structural model of its natural archetype, according to 2D  $^1\text{H}$ -NMR studies and molecular modeling. The effect of deprotonation of the axially coordinating imidazole ligand – as proposed for natural cofactor complexes – tunes significantly the position of the cathodic peak ( $\Delta V = -203$  mV) and stabilizes thereby the  $\text{Co}^{\text{III}}$  form. Partial deprotonation of the imidazole moiety through hydrogen bonding interactions was then achieved by immobilizing the biomimetic model on hydrophobic C18 silica, which yielded an unprecedented insight on how this class of Cbl-dependent proteins may fine-tune their properties in biological systems.

Received 17th November 2015

Accepted 23rd February 2016

DOI: 10.1039/c5sc04396d

www.rsc.org/chemicalscience

The vitamin  $\text{B}_{12}$  (“ $\text{B}_{12}$ ”) cofactors methylcobalamin (MeCbl) and adenosylcobalamin (AdoCbl) represent organometallic  $\text{Co}^{\text{III}}$ -corrinoids (Fig. 1 left) that catalyze biologically important methyl transfer and difficult [1, 2] rearrangement reactions.<sup>1</sup> In MeCbl-dependent enzymatic reactions, the cobalt–carbon bond of MeCbl is cleaved heterolytically, which generates a square planar Cob(II)alamin species. Alternatively, in the case of AdoCbl-dependent enzymes, homolytic bond scission leads to a protein bound cofactor in the  $\text{Co}^{\text{II}}$  state and an organic 5'-deoxyadenosyl radical (Ado $\cdot$ ). This difference in organometallic reactivity is remarkable, considering that MeCbl and AdoCbl cofactors share identical features, as (i) the redox-active cobalt ion, (ii) the equatorially chelating corrin ligand, (iii) the lower coordinating dimethylbenzimidazole (Dmbz) base and (iv) the upper cobalt–carbon bond (Fig. 1, left).<sup>2,3</sup> Obviously, a prominent role of the surrounding protein has been anticipated for triggering cobalt–carbon bond activation and enzymatic catalysis.<sup>4–9</sup>

In this context, most studies have focused so far on the impact of protein interactions with the upper axial ligand of the cofactor, whereas the interactions of the protein from the opposite site are less considered.<sup>10–14</sup> Indeed,  $\text{B}_{12}$  cofactors are anchored to  $\text{B}_{12}$ -dependent enzymes in two different ways: (i)

the cofactor retains its intramolecularly coordinating Dmbz base (“base-on” form) during cofactor incorporation into the protein (*e.g.* class II ribonucleotide reductase or diol dehydratase) or (ii) the intramolecularly coordinating Dmbz base of the cofactor is replaced by a protein histidine (“His”) anchoring group (“His-on” configuration). This mode of protein-cofactor binding is shown in Fig. 1 (ref. 10) and encountered, amongst others, in MeCbl-dependent methionine synthase (MetH) as well as AdoCbl dependent methylmalonyl CoA mutase (MCM) and glutamate mutase (GluM) (Table 1).<sup>15–17</sup>

Furthermore, the Co-bound His is part of a hydrogen-bonded amino acid chain, together with an aspartic acid (Asp) and a variable third residue (lysine for MCM or serine for MetH, Table 1).<sup>11,23</sup> The importance of the cofactor anchoring and the hydrogen bonding network for catalysis has been controversially discussed.<sup>13,23</sup> For example, mutation studies with MetH indicated a dramatic loss of activity while replacing either His or Asp by other amino acids in the hydrogen bonded network.<sup>23</sup> A different study focusing on “His-on” AdoCbl dependent isomerases indicate a structural reorganization of the hydrogen bonding network after substrate binding.<sup>13,24</sup> This behavior is suggested to stabilize the catalytically active cob(II)alamin intermediates by reducing the basicity of the anchoring His ligand.<sup>13</sup> Such behaviour seems very appealing and could represent a general mode of remote control in reactions depending on “His-on” configured cofactor  $\text{B}_{12}$ . Interestingly, a large number of heme-proteins such as globins, cytochromes c and horse radish peroxidase exhibit also a “His-on” type of

Department of Chemistry, University of Zurich, Winterthurerstr. 190, CH-8057, Zurich, Switzerland. E-mail: felix.zelder@chem.uzh.ch

† Electronic supplementary information (ESI) available. See DOI: 10.1039/c5sc04396d

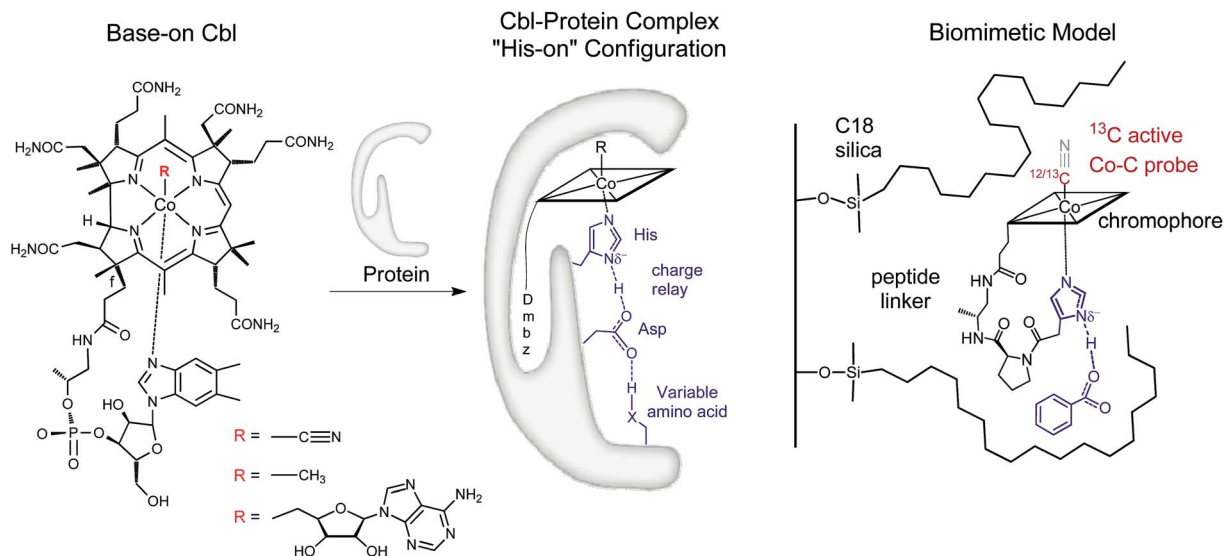


**Fig. 1** Left: Structure of vitamin  $\text{B}_{12}$  and Cbl cofactors having an intramolecularly bound dimethylbenzimidazole ("Dmbz") ("base-on") and distinct upper ligands ( $\text{R} = \text{CN}$ ,  $\text{B}_{12}$ ;  $\text{R} = \text{Me}$ ,  $\text{MeCbl}$ ;  $\text{R} = 5'$ -deoxyadenosyl,  $\text{AdoCbl}$ ). Middle: Cbl bound to the regulatory triad in the "histidine ("His")-on" form, as found in several  $\text{B}_{12}$ -dependent enzymes ( $\text{X} = \text{donor atom}$ , Table 1). Right: The corresponding biomimetic supramolecular model **1** with imidazole hydrogen-bonding interaction (charges are omitted).

cofactor attachment.<sup>25–28</sup> Partial deprotonation of the proximal His ligand within a lower part hydrogen bonding network enables the heme-dependent enzymes to fine-tune their properties and reactivity ("push effect").<sup>29–33</sup> This type of redox control has been thoroughly investigated for heme proteins, as the  $\text{Fe}^{\text{III}}\text{-}^{13}\text{CN}$  protoporphyrin IX complexes,<sup>34–36</sup> but was so far not studied for related mimics of "His on" Cbl@protein complexes.<sup>12,13,24,37–44</sup> In this context, only one example reported so far the heterogeneous model of a Cob(III)alamin–protein complex,<sup>14</sup> whereas some fascinating immobilized models of heme–protein complexes have recently attracted considerable attention.<sup>45–48</sup> Insights into the roles of the "His-on" cofactor attachment and the lower part hydrogen bonding network in  $\text{B}_{12}$ -dependent enzymes are therefore still required. In this context, the development of molecular mimics,<sup>13,40,42</sup> enzyme models<sup>44,49</sup> and new supramolecular biomimetic architectures<sup>14</sup> represent attractive assets.

We envisaged developing a new type of immobilized biomimetic model of the hydrogen bonding network, as found in "His-on"  $\text{B}_{12}$  cofactor complexes. This supramolecular assembly (Fig. 1 right) consists of three independent subunits: (i)

a structurally modified metal cofactor complex, (ii) a carboxylate ion and (iii) a hydrophobic silica C18 solid support. In particular, we envisaged to induce intermolecular hydrogen bonding between the immobilized  $\text{Co}^{\text{III}}$ -coordinated imidazole ligand and the carboxylate anion through hydrophobic interactions on the solid support.<sup>30</sup>

With this supramolecular immobilization strategy in mind, we began by developing the most important component of the supramolecular assembly: the molecular  $\text{B}_{12}$  derivative, mimicking the "His-on"  $\text{Co}^{\text{III}}$ -complex. This intramolecular coordination compound consists of three subunits: (i) the tetradentate  $\text{Co}^{\text{III}}$ -corrin complex, (ii) a lower ( $\alpha$ -) coordinating imidazole unit and (iii) a *trans*-located cyanide ligand (Fig. 1, right). Such a molecular model allows a thorough study of the imidazole-deprotonation influence on the redox properties (cyclic voltammetry), on the chromophore (UV-vis) and on the *trans*-influence exercised on the upper ( $\beta$ -) axial CN group ( $^{13}\text{C}$ -NMR). A meticulous structural modeling using QM/MM calculations (ESI, Fig. S1†) suggested the imidazole backbone derivative of  $\text{B}_{12}$  **1-H**<sup>+</sup> as a close biomimetic of the "His-on" configuration in  $\text{B}_{12}$ -cofactor protein complexes (Fig. 2).

**Table 1** Cbl ligation and lower part hydrogen bonding network in "His-on" configured  $\text{B}_{12}$  cofactor@protein complexes

Enzyme complex	Protein designation	Organism	Cofactor	Cofactor attachment and lower part hydrogen bonding network <sup>a</sup>	Reference
Methionine synthase	MetH	<i>Escherichia coli</i> , <i>Homo sapiens</i>	MeCbl	Asp-X- <u>His</u> -XX-Ser	18
Methylmalonyl CoA mutase	MCM	<i>Propionibacterium shermanii</i>	AdoCbl	Asp-X- <u>His</u> -XX-Lys	19 and 20
Glutamate mutase	GluM	<i>Homo sapiens</i> , <i>Ascaris lumbricoides</i> <i>Clostridium tetanomorphum</i> <i>Clostridium cochlearium</i>	AdoCbl	Asp-X- <u>His</u> -XX-Leu-X-Tyr <sup>b</sup>	21 and 22

<sup>a</sup> The cobalt anchoring group is underlined. <sup>b</sup> The Asp residue in GluM forms H-bonds with different residues (Leu and Tyr proposed here).

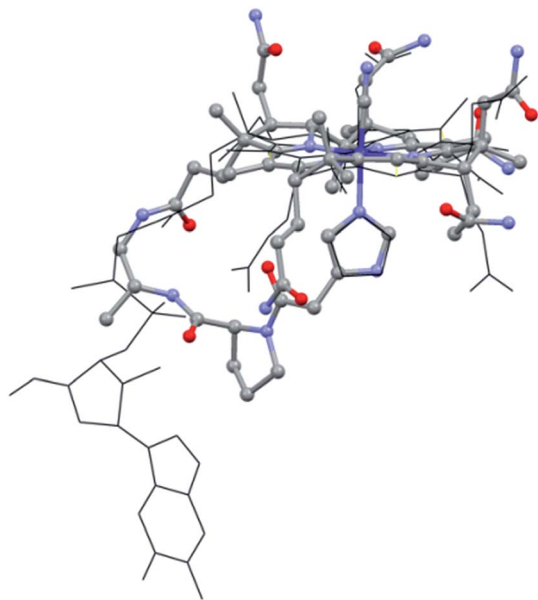


Fig. 2 Overlap of the "His-on" configuration in a B<sub>12</sub>-cofactor protein complex (wireframe; protein: MetH, only MeCbl and His shown, PDB: 1BMT)<sup>10</sup> and model of **1-H**<sup>+</sup> (ball and sticks).

In this compound, the imidazole subunit and the corrin macrocycle are connected *via* the *f*-side chain by an ethylenediamine spacer and a proline subunit.<sup>50–52</sup> **1-H**<sup>+</sup> was synthesized as trifluoroacetic acid (TFA) salt in three steps with an overall yield of 19% using common peptide coupling chemistry (ESI, Schemes S1 and S2†). The UV-vis spectrum of **1-H**<sup>+</sup> resembles that of vitamin B<sub>12</sub> (ESI, Fig. S2†), and the high resolution mass spectrum displays a signal at  $m/z = 610.30054$  (calculated:  $m/z = 610.30032$ ; [**1-H**<sup>+</sup> + H]<sup>2+</sup>).

The structural evaluation of the B<sub>12</sub>@protein model **1-H**<sup>+</sup> was investigated using 2D-ROESY. Through-space correlation was observed between H<sub>im</sub>2 (blue on Fig. 3) and the lower side chains 7A and 81 as well as the methyl group 51, all of which are situated at the northern face of the corrin ring. These interactions are complementary to correlations at the southern face of

the molecule, between H<sub>im</sub>5 and the corrin side chains 151, 131, as well as the 1R situated on the peptide backbone (red on Fig. 3). These data thus unambiguously indicate a coordination of the imidazole group through the N $\epsilon$ -nitrogen. These measurements also allowed determining the positioning of the imidazole unit with respect to the macrocycle, and revealed that it follows the C51–C151 axis of the corrin ring (Fig. 3B). Furthermore, comparison with the active site of a "His-on" bound B<sub>12</sub>-cofactor from crystal structure indicates a good agreement with the structural behavior of **1-H**<sup>+</sup> (Fig. 2).

Reversible proton release of **1-H**<sup>+</sup> (Scheme 1) was then tested by pH titration (from pH 8.5 to pH 12.5) and was detected with UV-vis spectroscopy. It revealed a bathochromic shift of 8 nm for both the  $\alpha$  and  $\beta$  bands (ESI, Fig. S3†) which indicates clearly that upon proton release, the imidazole moiety transforms to a stronger  $\sigma$ -donating imidazolate ligand.<sup>24,53–55</sup> Additionally, a pK<sub>a</sub> value of 10.8 was determined for N $\delta$  (ESI, Fig. S3†), which is about 4 pH units lower compared to free imidazole (pK<sub>a</sub> = 14.5)<sup>56</sup> and comparable to the values observed in His-anchored Fe<sup>III</sup>-<sup>13</sup>CN protoporphyrin IX@cytochrome *c* complexes (pK<sub>a</sub> = 10.1 to 10.6).<sup>36</sup>

The electrochemical properties of the cobalt center in **1-H**<sup>+</sup> and **1** were examined with cyclic voltammetry.<sup>57–59</sup> At pH 8.5, a cathodic peak at –920 mV vs. Ag/AgCl was observed for **1-H**<sup>+</sup> (Table 2, entry 2; Fig. S4†). We assign the cathodic wave to a two electron reduction of the octahedral coordinated Cob(III)alamin in a d<sup>6</sup>-electron configuration to a Co<sup>I</sup>-square planar complex in a d<sup>8</sup>-electron configuration, in agreement with electrochemical studies with B<sub>12</sub>.<sup>57,60</sup> Switching from compound **1-H**<sup>+</sup> to **1** (pH 12.5) with a Co<sup>III</sup>-coordinated imidazolate ligand significantly shifted the cathodic peak by 180 mV to a value of –1100 mV vs. Ag/AgCl (Table 2, entry 1; ESI, Fig. S4†). Deprotonation of **1-H**<sup>+</sup> to **1** thus stabilizes the Co<sup>III</sup> form against reduction.

The influence of the axial ligand basicity on the *trans*-located  $\beta$ -CN moiety was then investigated with NMR spectroscopy. The measurements were performed at two different pH (pH 7.0 and 12.5), with an isotopically labeled <sup>13</sup>CN ligand on the  $\beta$ -side of the cobalt. The <sup>13</sup>C-NMR of **1-H**<sup>+</sup> revealed a broad signal at

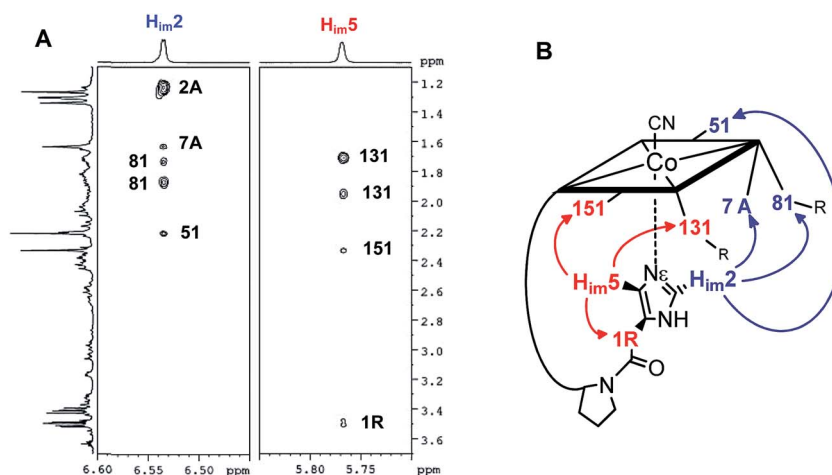
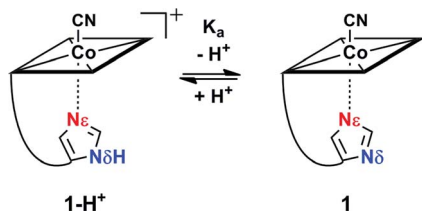


Fig. 3 (A): 2D-ROESY coupling of **1-H**<sup>+</sup> (B): the corresponding correlation in the structure (in D<sub>2</sub>O, 270 K, 500 MHz) (charge is omitted).



Scheme 1 pH equilibrium between  $1\text{-H}^+$  and  $1$ .

127 ppm ( $^{13}\text{C}$ N moiety) which shifts downfield (133 ppm) upon deprotonation ( $1$ ) (ESI, Fig. S5†). This behavior is explained by the coordination of a stronger  $\sigma$ -donor (imidazolate,  $1$ ), which results in a decreased polarization of the *trans*-located cyanide  $\pi$ -electron density.<sup>61,62</sup> The broadening of the  $^{13}\text{C}$ N lines of  $1$  and  $1\text{-H}^+$  (375 vs. 150 Hz) is due to the distinct nuclear quadrupolar properties of  $^{59}\text{Co}$ , which significantly increase the  $t_1$  and  $t_2$  relaxation rates of the directly bound carbon. These effects also prevent the observation of resolved  $^{13}\text{C}$ -multiplets due to scalar coupling between  $^{13}\text{C}$  and  $^{59}\text{Co}$ . Other broadening mechanisms like anisotropic effects or paramagnetic impurities can be excluded, because all remaining  $^{13}\text{C}$  resonances of the measured compounds are sharp (ESI, Fig. S5†).

Control experiments (CV, UV-vis,  $^{13}\text{C}$ -NMR) were performed with a 'blocked' model at pH 7.0 and pH 12.5 in the same manner described for  $1\text{-H}^+$  and  $1$  (ESI, Fig. S6†).  $\text{B}_{12}$  was used for this purpose, since it contains an  $\alpha$ -coordinating Dmbz ligand resembling the imidazole unit, for which reversible protonation of both nitrogens is impossible (Fig. 1, left). In effect, all control experiments with  $\text{B}_{12}$  exhibited no significant shifts upon pH changes, thus proving that all results obtained with  $1\text{-H}^+$  and  $1$  originated from the deprotonation of the imidazole ligand.

Plotting the position of the cathodic peak  $E_{\text{pc}}$  against the upper cyanide  $^{13}\text{C}$ -NMR shift for the 'blocked' model  $\text{B}_{12}$ , the biomimetic compounds  $1$  and  $1\text{-H}^+$  as well as two other compounds which present distinct lower axial ligand (aquacyanocobinamide, aquaCNCbi; Fig. 4, right; and dicyanocobinamide, diCNCbi; Fig. 4, right) gives a more extensive picture on the influence of lower ligand modulation (Fig. 4).<sup>13,24,64,65</sup> The linear correlation suggests that the relative  $\sigma$ -donating capacities of the lower ligand similarly influence both the cathodic peak ( $E_{\text{pc}}$ ) and the upper CN  $^{13}\text{C}$  shift. Furthermore, by considering that aquaCNCbi represents a model for base-off  $\text{B}_{12}$ , important insights are extracted on how Cbls and Cbl@protein complexes may alter their electrochemical

properties in biological systems. Indeed, when considering  $\text{B}_{12}$  alone, the tuning of the redox properties is reached only through the "base-on/base-off" switch, where the  $\alpha$ -Dmbz ligand is replaced by the weaker electron donating  $\text{H}_2\text{O}$  molecule. However, this modification only leads to the destabilization of the cobalt center, as shown by the less negative  $E_{\text{pc}}$  value for the  $\text{Co}(\text{II})/\text{Co}(\text{I})$  reduction of aquaCNCbi ( $E_{\text{pc}} = -749$  mV vs. Ag/AgCl, Table 2, entry 4). The contrary effect, a stabilization of the metal ion seems not to be possible in this coordination mode. Switching the  $\alpha$ -Dmbz ligand of  $\text{B}_{12}$  to an imidazole moiety, as encountered in  $1\text{-H}^+$ , exhibits only a small effect on the  $\text{Co}(\text{III})/\text{Co}(\text{I})$  reduction ( $\Delta V = -23$  mV, Table 2, entry 2 and 3). However, deprotonation to an imidazolate moiety ( $1$ ) is now possible and leads to a substantial cathodic shift of  $-203$  mV (Table 2, entry 1–3). The lower ligand modulation of  $1\text{-H}^+$  thus leads to a doubling of the available redox range (Fig. 4,  $-749$  to  $-1100$  mV vs. Ag/AgCl) compared to  $\text{B}_{12}$  alone (Fig. 4,  $-749$  to  $-897$  mV vs. Ag/AgCl). This behavior underscores strikingly that (partial) deprotonation of the coordinated His-residue offers  $\text{B}_{12}$ -dependent proteins an elegant tool for fine-tuning their electron donating properties on demand. The lower ligand modulation is also reflected in a bathochromic shift of the  $\alpha$ -band (Table 2) and the  $\beta$ -band wavelengths (data not shown). Furthermore, linear correlations are observed between the  $E_{\text{pc}}$  and the  $\alpha$ -band (Fig. 4) or the  $\beta$ -band (data not shown). This behavior is in line with recent spectroscopic and theoretical studies, which show that the position of the  $\alpha$ -band reflects the  $d_{22}$  contribution of the lower coordinating ligand to the HOMO orbital.<sup>24,53–55</sup>

In His-on Cbl complexes, the deprotonation of the His residue is achieved through an H-bonded chain in between the ligand triad. However, under aqueous conditions, deprotonation was only achieved at pH values above the  $\text{p}K_{\text{a}}$  of  $1\text{-H}^+$  (10.8). For mimicking the biological situation with the model  $1\text{-H}^+$  more closely, we thus decided to investigate the interactions between the imidazole of  $1\text{-H}^+$  and an exogenous carboxylate as H-bonding acceptor. For this purpose, we applied first benzoic acid in dioxane- $\text{H}_2\text{O}$  mixtures of  $1\text{-H}^+$ ,<sup>67</sup> which did not result in any spectroscopic changes. Immobilized  $1\text{-H}^+$  ( $1\text{-H}^+_{\text{SP}}$ ) on C18 silica material behaved differently and allowed studying proton release with diffuse reflectance spectroscopy, an approach recently introduced by our group.<sup>14</sup>

$1\text{-H}^+_{\text{SP}}$  remains base-on upon immobilization, as indicated by the characteristic reflectance spectrum of a "base-on" Cbl (ESI, Fig. S7†). In agreement with studies under homogenous

Table 2  $E_{\text{pc}}$ ,  $^{13}\text{C}$ N shift and position of the  $\alpha$ -band of different  $\text{B}_{12}$  derivatives

Entry	Compound	$E_{\text{pc}}^a$ (mV)	CN $^{13}\text{C}$ -NMR shift <sup>d</sup> (ppm)	$\lambda$ of $\alpha$ -band <sup>f</sup> (nm)
1	$1$	$-1100^b$	133	563
2	$1\text{-H}^+$	$-920^b$	127	556
3	$\text{B}_{12}$	$-897^b$	124	551
4	aquaCNCbi	$-749^c$	112 <sup>e</sup>	530
5	diCNCbi	$-1170^b$	139 <sup>e</sup>	580

<sup>a</sup> vs. Ag/AgCl, 1.5 mM in 0.1 M KCl, scan rate:  $0.005 \text{ V s}^{-1}$ . <sup>b</sup>  $E_{\text{pc}}$  for the  $\text{Co}(\text{III})/\text{Co}(\text{I})$  reduction. <sup>c</sup>  $E_{\text{pc}}$  for the  $\text{Co}(\text{II})/\text{Co}(\text{I})$  reduction. <sup>d</sup> In  $\text{D}_2\text{O}$ ; 126 MHz.

<sup>e</sup> Values obtained from ref. 63. <sup>f</sup> In  $\text{H}_2\text{O}$ .



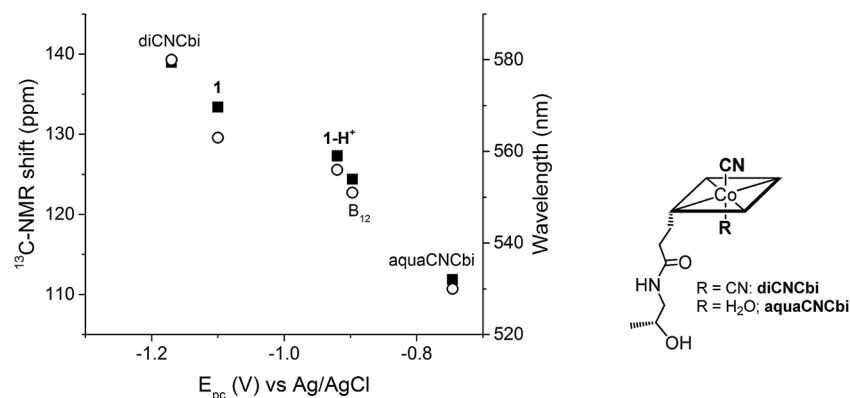


Fig. 4 Left: Correlation between  $E_{pc}$  ( $\text{Co}^{\text{III}}/\text{Co}^{\text{I}}$  reduction for all compounds, except aquaCNCbi:  $\text{Co}^{\text{II}}/\text{Co}^{\text{I}}$  reduction) and the  $^{13}\text{C}$ -NMR shift of CN (left axis, ■) and the  $\alpha$ -band wavelength (right axis, ○); B<sub>12</sub> data correspond to both pH 7.0 and pH 12.5. Right: Structure of aquaCNCbi and diCNCbi (charges are omitted).<sup>66</sup>

conditions, treatment of  $1\text{-H}_{\text{sp}}^+$  with a strong base (1 M NaOH) led to a bathochromic shift (6 nm for the  $\alpha$ -band) and indicated imidazole deprotonation (Fig. 5; ESI, Fig. S7<sup>†</sup>). However, the addition of pure toluene, which lacks any H-bond acceptor, to  $1\text{-H}_{\text{sp}}^+$  did not lead to any changes. In contrast, the further addition of benzoate (tetrabutylammonium salt) to this solvent led to a slight, but characteristic bathochromic shift of the  $\alpha$ -band (4 nm) and  $\beta$ -band (2 nm) (Fig. 5; ESI, Fig. S8<sup>†</sup>), which suggests hydrogen-bonding between benzoate and the N $\delta$

hydrogen of  $1\text{-H}_{\text{sp}}^+$ , similar to the situation proposed for this class of proteins.<sup>10,13</sup>

In summary, we present an unprecedented supramolecular assembly mimicking the regulatory ligand triad of “His-on” metal-cofactor@protein complexes. The data presented herein give evidence that deprotonation of an axially coordinating imidazole to form imidazolate stabilizes significantly ( $\Delta V = -203$  mV) the  $\text{Co}^{\text{III}}$  form of the corrinoid. However, such behavior cannot be achieved with B<sub>12</sub> in its base-on form.

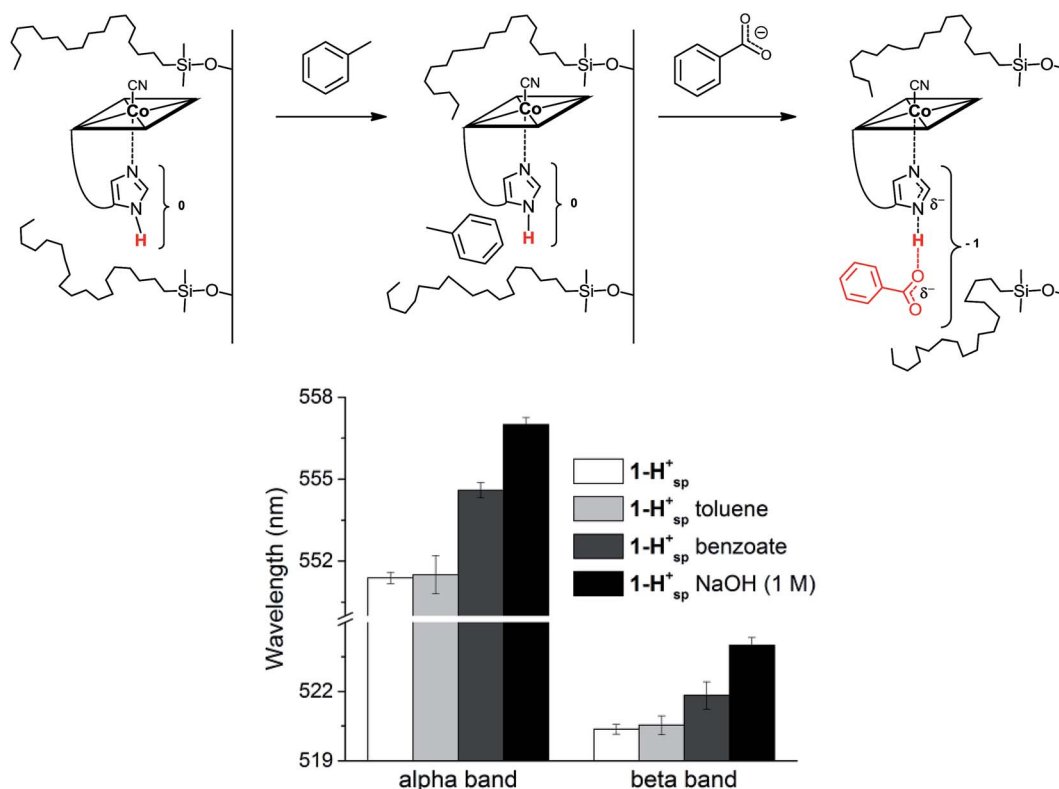


Fig. 5 Top: Proposed mechanism for the reaction of  $1\text{-H}_{\text{sp}}^+$  immobilized on C18 silica (left) with toluene (middle) and with benzoate (tetra-butylammonium salt; right). Bottom: Absorbance for the  $\alpha$  and  $\beta$  bands of immobilized  $1\text{-H}_{\text{sp}}^+$  (white),  $1\text{-H}_{\text{sp}}^+$  after the addition of toluene (light grey),  $1\text{-H}_{\text{sp}}^+$  after the addition of a solution of benzoate in toluene (dark grey) and  $1\text{-H}_{\text{sp}}^+$  after the addition of 1 M NaOH (black) ( $n = 4$ ) (charges are omitted).



Modulating the corrinoid redox properties with this elegant trick represents therefore a sophisticated strategy for tailoring the electronic properties of Cbls in biological systems.

## Acknowledgements

The authors thank L. Bigler for the recording of the HR-ESI-MS spectra, C. Männel-Croisé for help with the DRUV-Vis measurements and R. Alberto for support. A generous gift of vitamin B<sub>12</sub> from DSM Nutritional Products AG (Basel/Switzerland) is acknowledged. This work was supported by the Swiss National Science Foundation (Grant No. 200020-149108).

## References

- 1 K. Gruber, B. Puffer and B. Kräutler, *Chem. Soc. Rev.*, 2011, **40**, 4346–4363.
- 2 R. Banerjee, *Chemistry and Biochemistry of B12*, Wiley-Interscience, New York, 1st edn, 1999.
- 3 F. Zelder, *Chem. Commun.*, 2015, **51**, 14004–14017.
- 4 P. Friedrich, U. Baisch, R. W. Harrington, F. Lyatuu, K. Zhou, F. Zelder, W. McFarlane, W. Buckel and B. T. Golding, *Chem.-Eur. J.*, 2012, **18**, 16114–16122.
- 5 A. J. Brooks, C. C. Fox, E. N. G. Marsh, M. Vlasie, R. Banerjee and T. C. Brunold, *Biochemistry*, 2005, **44**, 15167–15181.
- 6 A. J. Brooks, M. Vlasie, R. Banerjee and T. C. Brunold, *J. Am. Chem. Soc.*, 2004, **126**, 8167–8180.
- 7 D. Bucher, G. M. Sandala, B. Durbeej, L. Radom and D. M. Smith, *J. Am. Chem. Soc.*, 2012, **134**, 1591–1599.
- 8 J. Masuda, N. Shibata, Y. Morimoto, T. Toraya and N. Yasuoka, *Structure*, 2000, **8**, 775–788.
- 9 A. M. Calafat and L. G. Marzilli, *J. Am. Chem. Soc.*, 1993, **115**, 9182–9190.
- 10 C. L. Drennan, S. Huang, J. T. Drummond, R. G. Matthews and M. L. Ludwig, *Science*, 1994, **266**, 1669–1674.
- 11 J. T. Jarrett, C. Y. Choi and R. G. Matthews, *Biochemistry*, 1997, **36**, 15739–15748.
- 12 J. M. Puckett, M. B. Mitchell, S. Hirota and L. G. Marzilli, *Inorg. Chem.*, 1996, **35**, 4656–4662.
- 13 K. S. Conrad, C. D. Jordan, K. L. Brown and T. C. Brunold, *Inorg. Chem.*, 2015, **54**, 3736–3747.
- 14 C. Männel-Croisé and F. Zelder, *Chem. Commun.*, 2011, **47**, 11249–11251.
- 15 W. Buckel and B. T. Golding, *Chem. Soc. Rev.*, 1996, **25**, 329–337.
- 16 S. Dong, R. Padmakumar, N. Maiti, R. Banerjee and T. G. Spiro, *J. Am. Chem. Soc.*, 1998, **120**, 9947–9948.
- 17 K. L. Brown, *Chem. Rev.*, 2005, **105**, 2075–2149.
- 18 R. G. Matthews, M. Koutmos and S. Datta, *Curr. Opin. Struct. Biol.*, 2008, **18**, 658–666.
- 19 R. Banerjee and S. Chowdhury, in *Chemistry and Biochemistry of B12*, ed. R. Banerjee, Wiley-Interscience, New York, 1st edn, 1999, pp. 707–730.
- 20 F. Mancia, N. H. Keep, A. Nakagawa, P. F. Leadlay, S. McSweeney, B. Rasmussen, O. Diat and P. R. Evans, *Structure*, 1996, **4**, 339–350.
- 21 W. Buckel, G. Bröker, H. Bothe, A. J. Pierik and B. T. Golding, in *Chemistry and Biochemistry of B12*, ed. R. Banerjee, Wiley-Interscience, New York, 1st edn, 1999, pp. 757–782.
- 22 R. Reitzer, K. Gruber, G. Jögl, U. G. Wagner, H. Bothe, W. Buckel and C. Kratky, *Structure*, 1999, **7**, 891–902.
- 23 J. T. Jarrett, M. Amaratunga, C. L. Drennan, J. D. Scholten, R. H. Sands, M. L. Ludwig and R. G. Matthews, *Biochemistry*, 1996, **35**, 2464–2475.
- 24 T. A. Stich, A. J. Brooks, N. R. Buan and T. C. Brunold, *J. Am. Chem. Soc.*, 2003, **125**, 5897–5914.
- 25 U. Ermler, R. A. Siddiqui, R. Cramm and B. Friedrich, *EMBO J.*, 1995, **14**, 6067–6077.
- 26 J. D. Satterlee and J. E. Erman, *Biochemistry*, 1991, **30**, 4398–4405.
- 27 J. H. Dawson, *Science*, 1988, **240**, 433–439.
- 28 T. Spiro, *ACS Chem. Biol.*, 2008, **3**, 673–675.
- 29 D. B. Goodin and D. E. McRee, *Biochemistry*, 1993, **32**, 3313–3324.
- 30 D. Nonaka, H. Wariishi, K. G. Welinder and H. Fujii, *Biochemistry*, 2010, **49**, 49–57.
- 31 T. G. Spiro, G. Smulevich and C. Su, *Biochemistry*, 1990, **29**, 4497–4508.
- 32 V. P. Chacko and G. N. La Mar, *J. Am. Chem. Soc.*, 1982, **104**, 7002–7007.
- 33 L. Banci, I. Bertini, P. Turano, M. Tien and T. K. Kirk, *Proc. Natl. Acad. Sci. U. S. A.*, 1991, **88**, 6956–6960.
- 34 H. Fujii, *J. Am. Chem. Soc.*, 2002, **124**, 5936–5937.
- 35 H. Fujii and T. Yoshida, *Inorg. Chem.*, 2006, **45**, 6816–6827.
- 36 S. E. Bowman and K. L. Bren, *Inorg. Chem.*, 2010, **49**, 7890–7897.
- 37 L. Banci, A. Rosato and P. Turano, *J. Biol. Inorg. Chem.*, 1996, **1**, 364–367.
- 38 C. Olea Jr, J. Kuriyan and M. A. Marletta, *J. Am. Chem. Soc.*, 2010, **132**, 12794–12795.
- 39 S. Hirota, S. M. Polson, J. M. Puckett, S. J. Moore, M. B. Mitchell and L. G. Marzilli, *Inorg. Chem.*, 1996, **35**, 5646–5653.
- 40 S. J. Moore, A. Kutikov, R. J. Lachicotte and L. G. Marzilli, *Inorg. Chem.*, 1999, **38**, 768–776.
- 41 M. Fasching, W. Schmidt, B. Krautler, E. Stupperich, A. Schmidt and C. Kratky, *Helv. Chim. Acta*, 2000, **83**, 2295–2316.
- 42 B. Kräutler, *Öster. Chem. Zeit.*, 1989, 2–9.
- 43 M. Kumar and P. M. Kozlowski, *Chem. Commun.*, 2012, **48**, 4456–4458.
- 44 T. Hayashi, Y. Morita, E. Mizohata, K. Oohora, J. Ohbayashi, T. Inoue and Y. Hisaeda, *Chem. Commun.*, 2014, **50**, 12560–12563.
- 45 M. Bröring, *Angew. Chem., Int. Ed.*, 2007, **46**, 6222–6224.
- 46 J. P. Collman, N. K. Devaraj, R. A. Decréau, Y. Yang, Y.-L. Yan, W. Ebina, T. A. Eberspacher and C. E. D. Chidsey, *Science*, 2007, **315**, 1565–1568.
- 47 T. Itoh, K. Yano, T. Kajino, Y. Inada and Y. Fukushima, *Biotechnol. Bioeng.*, 2006, **93**, 476–484.
- 48 A. Hosseini, C. J. Barile, A. Devadoss, T. A. Eberspacher, R. A. Decreau and J. P. Collman, *J. Am. Chem. Soc.*, 2011, **133**, 11100–11102.



- 49 Y. Morita, K. Oohora, A. Sawada, K. Doitomi, J. Ohbayashi, T. Kamachi, K. Yoshizawa, Y. Hisaeda and T. Hayashi, *Dalton Trans.*, 2016, **45**, 3277–3284.
- 50 K. Zhou and F. Zelder, *Angew. Chem., Int. Ed.*, 2010, **49**, 5178–5180.
- 51 F. Zelder, K. Zhou and M. Sonnay, *Dalton Trans.*, 2013, **42**, 854–862.
- 52 K. ó. Proinsias, M. Giedyk and D. Gryko, *Chem. Soc. Rev.*, 2013, **42**, 6605–6619.
- 53 J. M. Pratt, in *Inorganic Chemistry of Vitamin B12*, ed. J. M. Pratt, Academic Press, New York, 1972, p. 44.
- 54 T. Andruniow, P. M. Kozlowski and M. Z. Zgierski, *J. Chem. Phys.*, 2001, **115**, 7522–7533.
- 55 R. A. Firth, H. A. O. Hill, J. M. Pratt, R. J. P. Williams and W. R. Jackson, *Biochemistry*, 1967, **6**, 2178–2189.
- 56 T. Eicher and S. Hauptmann, *The Chemistry of Heterocycles: Structures, Reactions, Synthesis, and Applications 2nd*, John Wiley & Sons, 2003.
- 57 D. Lexa and J. M. Saveant, *Acc. Chem. Res.*, 1983, **16**, 235–243.
- 58 C. Costentin, G. Passard, M. Robert and J.-M. Savéant, *Chem. Sci.*, 2013, **4**, 819–823.
- 59 I. A. Dereven'kov, D. S. Salnikov, R. Silaghi-Dumitrescu, S. V. Makarov and O. I. Koifman, *Coord. Chem. Rev.*, 2016, **309**, 68–83.
- 60 D. Lexa, J. M. Sayeant and J. Zickler, *J. Am. Chem. Soc.*, 1980, **102**, 2654–2663.
- 61 P. L. Gaus and A. L. Crumbliss, *Inorg. Chem.*, 1976, **15**, 739–741.
- 62 R. A. Firth, H. A. O. Hill, J. M. Pratt, R. G. Thorp and R. J. P. Williams, *J. Chem. Soc. A*, 1968, 2428–2433.
- 63 K. L. Brown, in *Chemistry and Biochemistry of B12*, ed. R. Banerjee, Wiley-Interscience, New York, 1st edn, 1999, pp. 197–238.
- 64 A. J. Reig, K. S. Conrad and T. C. Brunold, *Inorg. Chem.*, 2012, **51**, 2867–2879.
- 65 K. L. Brown, *Dalton Trans.*, 2006, 1123–1133.
- 66 G. L. Nelsestuen, T. H. Zytkevich and J. B. Howard, *J. Biol. Chem.*, 1974, **249**, 6347–6350.
- 67 M. Komiyama, M. L. Bender, M. Utaka and A. Takeda, *Proc. Natl. Acad. Sci. U. S. A.*, 1977, **74**, 2634–2638.

